university of groningen

University Medical Center Groningen

University of Groningen

Regulation of archaella expression by the FHA and von Willebrand domain-containing proteins ArnA and ArnB in Sulfolobus acidocaldarius

Reimann, Julia; Lassak, Kerstin; Khadouma, Sunia; Ettema, Thijs J. G.; Yang, Nuan; Driessen, Arnold J. M.; Klingl, Andreas; Albers, Sonja-Verena

Published in:
Molecular Microbiology

DOI:
10.1111/j.1365-2958.2012.08186.x

IMPORTANT NOTE: You are advised to consult the publisher's version (publisher's PDF) if you wish to cite from it. Please check the document version below.

Document Version
Publisher's PDF, also known as Version of record

Publication date:
2012

Link to publication in University of Groningen/UMCG research database

Citation for published version (APA):
Reimann, J., Lassak, K., Khadouma, S., Ettema, T. J. G., Yang, N., Driessen, A. J. M., Klingl, A., & Albers, S-V. (2012). Regulation of archaella expression by the FHA and von Willebrand domain-containing proteins ArnA and ArnB in Sulfolobus acidocaldarius. *Molecular Microbiology*, *86*(1), 24-36. https://doi.org/10.1111/j.1365-2958.2012.08186.x

Copyright
Other than for strictly personal use, it is not permitted to download or to forward/distribute the text or part of it without the consent of the author(s) and/or copyright holder(s), unless the work is under an open content license (like Creative Commons).

The publication may also be distributed here under the terms of Article 25fa of the Dutch Copyright Act, indicated by the “Taverne” license. More information can be found on the University of Groningen website: https://www.rug.nl/library/open-access/self-archiving-pure/taverne-amendment.

Take-down policy
If you believe that this document breaches copyright please contact us providing details, and we will remove access to the work immediately and investigate your claim.

Downloaded from the University of Groningen/UMCG research database (Pure): http://www.rug.nl/research/portal. For technical reasons the number of authors shown on this cover page is limited to 10 maximum.

Molecular Microbiology (2012) 86(1), 24–36 ■
doi:10.1111/j.1365-2958.2012.08186.x
First published online 22 August 2012

Regulation of archaella expression by the FHA and von Willebrand domain-containing proteins ArnA and ArnB in *Sulfolobus acidocaldarius*

Julia Reimann,[1] Kerstin Lassak,[1] Sunia Khadouma,[1] Thijs J. G. Ettema,[2] Nuan Yang,[3] Arnold J. M. Driessen,[3] Andreas Klingl[4] and Sonja-Verena Albers[1]*

[1]*Max Planck Institute for Terrestrial Microbiology, Molecular Biology of Archaea, Karl-von-Frisch-Strasse 10, 35043 Marburg, Germany.*
[2]*Department of Molecular Evolution, Biomedical Center, Uppsala University, Husargatan 3, SE-75237 Uppsala, Sweden.*
[3]*Groningen Biomolecular Sciences and Biotechnology Institute and Zernike Institute for Advanced Materials, University of Groningen, Nijenborgh 7, 9747 AG Groningen, the Netherlands.*
[4]*Cell Biology and LOEWE Research Centre for Synthetic Microbiology, Phillipps University Marburg, Karl-von-Frisch-Strasse 8, 35032 Marburg, Germany.*

Summary

The ability of microorganisms to sense and respond to sudden changes in their environment is often based on regulatory systems comprising reversible protein phosphorylation. The archaellum (former: archaeal flagellum) is used for motility in Archaea and therefore functionally analogous to the bacterial flagellum. In contrast with archaellum-mediated movement in certain members of the Euryarchaeota, this process, including its regulation, remains poorly studied in crenarchaeal organisms like *Sulfolobus* species. Recently, it was shown in *Sulfolobus acidocaldarius* that tryptone limiting conditions led to the induction of archaella expression and assembly. Here we have identified two proteins, the FHA domain-containing protein ArnA and the vWA domain-containing protein ArnB that are involved in regulating archaella expression in *S. acidocaldarius*. Both proteins are phosphorylated by protein kinases *in vitro* and interact strongly *in vivo*. Phenotypic analyses revealed that these two proteins are repressors of archaella expression. These results represent the first step in understanding the networks that underlie regulation of cellular motility in Crenarchaeota and emphasize the importance of protein phosphorylation in the regulation of cellular processes in the Archaea.

Accepted 24 July, 2012. *For correspondence. E-mail albers@mpi-marburg.mpg.de; Tel. (+49) 6421178426; Fax (+49) 6421178429.

© 2012 Blackwell Publishing Ltd

Introduction

All microorganisms have to withstand and respond to sudden changes in their environment. The availability of nutrient sources is sensed to regulate metabolic pathways and to detect nutrient limiting conditions. Therefore, perception of extracellular stimuli and their transduction in the cell is essential for survival of microorganisms. Chemotaxis sensory systems link the signal input to motility, allowing microorganisms to escape hostile environments. Chemotaxis systems have been well studied in Bacteria, in which signals sensed by a chemoreceptor are always transduced to a two-component signal transduction pathway, which modulates flagella movement upon binding of phosphorylated CheY-P to the flagellar motor switch protein FliM (Welch *et al*., 1993; Dyer *et al*., 2009). Among Archaea, only the Euryarchaeota possess such a bacterial-like chemotaxis system, which is best studied in *Halobacterium salinarum* (Rudolph *et al*., 1995; Rudolph and Oesterhelt, 1996). However, the archaellum [former the archaeal flagellum (Jarrell and Albers, 2012)] is only functionally, but not structurally related to the bacterial flagellum, as it is evolutionary related to bacterial type IV pili. Two core subunits of the archaellum, the ATPase FlaI and the integral membrane protein FlaJ, are homologues of PilB and PilC in bacterial type IV pili (Pohlschroder *et al*., 2011). Moreover, the processing of the archaellins, the structural subunits of the archaellum, prior to assembly is conserved in bacterial type IV pilins (Pohlschroder *et al*., 2011). Therefore the final step in regulating archaella-mediated movement upon CheY-P interaction is envisioned to differ from the bacterial flagella system. In *H. salinarum* three proteins (two of the DUF439 family, CheM, and one of the HEAT_PBS family) were identified that bind the chemotaxis proteins CheY, CheD and CheC2 as well as the archaella proteins FlaCE and FlaD. Hence, these proteins

seemingly connect the sensory system to the motility system in this organism (Schlesner *et al*., 2009; Alatyrev *et al*., 2010). In *Methanococcus jannaschii* and *M. maripaludis* archaella expression increased at low hydrogen concentrations and additionally was reduced during leucine limitation in *M. maripaludis* (Mukhopadhyay *et al*., 2000; Hendrickson *et al*., 2008). However, how archaella regulation is achieved in Crenarchaeota is not understood, as information about the regulatory pathways and the inducing conditions is not available. Homologues of chemotaxis proteins have not been identified in the Crenarchaeota so far. Recently, it was shown that in *Sulfolobus acidocaldarius*, one of the main crenarchaeal model organisms, tryptone limiting conditions led to the induction of archaella expression and assembly (Lassak *et al*., 2012). However, the factors involved in regulation of this process are still unknown.

Forkhead-associated (FHA) domains were first described as modules occurring in forkhead transcription factors (Hofmann and Bucher, 1995). Since then, FHA domain-containing proteins were structurally and functionally analysed in detail revealing a phosphopeptide-binding activity with a clear specificity towards p-Thr over p-Ser or p-Tyr (Durocher *et al*., 2000; Pennell *et al*., 2010). Because of these specific interactions FHA domains, which are found in all three domains of life, are important modules in phosphopeptide-mediated processes in the cell like signal transduction and DNA damage response pathways. Most studies on FHA domains were conducted in Eukaryotes or Bacteria, whereas 33 of these phosphopeptide-specific binding proteins are predicted in archaeal genomes (http://smart.embl-heidelberg.de/). FHA domain-containing proteins not only bind phosphopeptides, but can also be phosphorylated *in vitro* by eukaryotic-like protein kinases (ePKs) that are distantly encoded on the genome in *Mycobacterium tuberculosis* (Grundner *et al*., 2005). A similar result was shown for the crenarchaeal *Sulfolobus tokodaii* FHA protein, which was phosphorylated *in vitro* by a Serine/Threonine PK and binds the archaellar *flaX* promoter in a phosphorylation-dependent manner (Wang *et al*., 2010; Duan and He, 2011). Strikingly, in *Sulfolobus* spp. these FHA proteins always seem to be present in an operon with a gene encoding for a von Willebrand domain-containing protein (vWA). Primarily, the von Willebrand type A domain of about 200 amino acids was found in the von Willebrand factor, a protein secreted to the blood plasma in mammals (Sadler *et al*., 1985). The most ancient vWA proteins are now known to be intracellular proteins. These proteins are encoded in all three domains of life and are involved in different processes like signal transduction, cell adhesion and migration (Colombatti *et al*., 1993; Whittaker and Hynes, 2002). A common feature of vWA proteins is to form multi-protein complexes (Tuckwell, 1999; Whittaker and Hynes, 2002). However, in archaea these domains have not been functionally characterized.

In this study we have analysed the role of the FHA protein ArnA and the vWA domain-containing protein ArnB in the regulation of the archaellum operon in *S. acidocaldarius*. Both proteins were phosphorylated by specific ePKs and interacted strongly *in vivo*. Genetic analyses showed that these two proteins are repressors of archaella expression. These results represent the first step in understanding regulatory networks in Crenarchaea and underline the importance of protein phosphorylation in cellular processes in the Archaea.

Results

The arn *cluster and its evolution*

Interestingly, each member of the *Sulfolobales* contains only one FHA protein in its genome, which displays an N-terminal predicted Zinc finger domain. In *S. acidocaldarius* the FHA protein is encoded in an operon with one of the three vWA-containing proteins that are present in the *S. acidocaldarius* genome (Fig. 1A). Later on we demonstrate that these two proteins are part of the *archaellum regulatory network* and term these proteins as ArnA and ArnB (Fig. 1A). A comparative genome analysis revealed that the *S. acidocaldarius arn* cluster is conserved across a number of *Sulfolobus* species (Fig. 1B). The gene cluster invariably encodes an FHA domain-comprising gene and one copy of a gene encoding a vWA domain-containing protein. In the *Sulfolobales* this cluster is flanked upstream by a second vWA protein encoded in the opposite direction. Additionally, a gene encoding a protein with a predicted protein phosphatase activity seems to be part of the gene cluster in some cases, but this is not observed for *S. acidocaldarius* and *S. tokodaii*, where these genes are encoded at a distinct region on the chromosome (*saci0884* respectively *ST2367*) (Fig. 1B). The presence of two gene copies of the vWA domain-containing proteins is best explained by an ancient gene duplication event at the base of the *Sulfolobales*, followed by lineage-specific gene loss and/or horizontal gene transfer events in the branches leading towards *Metallosphaera*. The presence of the *arn* gene cluster in *Picrophilus torridus* is most likely the result of a horizontal gene transfer event given that this is the only species of the Euryarchaeota that contains the gene cluster (Fig. 1C).

Interestingly, a variant of the *arn* gene cluster seems to be present in certain members of the *Desulfurococcales* (*Pyrolobus fumarii* and *Staphylothermus* spp.). In which these gene clusters do contain the FHA- and vWA-containing genes, the protein phosphatase-encoding gene seems to be displaced by an unrelated Serine/Threonine protein kinase of the Pkinase superfamily (PFAM00069)

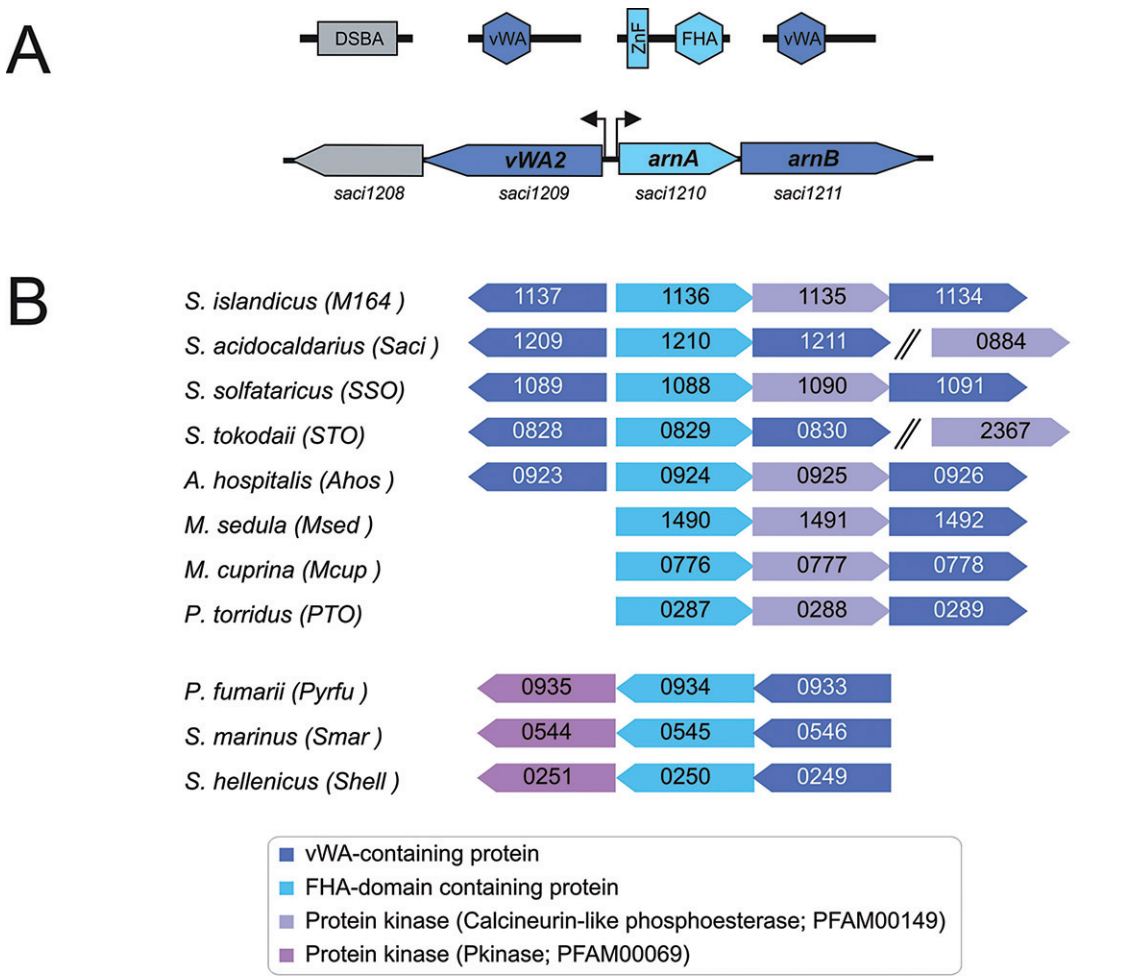
A
DSBA
vWA
ZnF
FHA
vWA
vWA2
arnA
arnB
saci1208
saci1209
saci1210
saci1211
B
S. islandicus (M164)
1137
1136
1135
1134
S. acidocaldarius (Saci)
1209
1210
1211
0884
S. solfataricus (SSO)
1089
1088
1090
1091
S. tokodaii (STO)
0828
0829
0830
2367
A. hospitalis (Ahos)
0923
0924
0925
0926
M. sedula (Msed)
1490
1491
1492
M. cuprina (Mcup)
0776
0777
0778
P. torridus (PTO)
0287
0288
0289
P. fumarii (Pyrfu)
0935
0934
0933
S. marinus (Smar)
0544
0545
0546
S. hellenicus (Shell)
0251
0250
0249
vWA-containing protein
FHA-domain containing protein
Protein kinase (Calcineurin-like phosphoesterase; PFAM00149)
Protein kinase (Pkinase; PFAM00069)
C
Ahos_0923 Acidianus hospitalis
SSO1089 Sulfolobus solfataricus
M1425_1137 Sulfolobus islandicus
ST0828 Sulfolobus tokodaii
Saci_1209 Sulfolobus acidocaldarius
SSO1091 Sulfolobus solfataricus
M1425_1134 Sulfolobus islandicus
Mcup_0778 Metallosphaera cuprina
Msed_1492 Metallosphaera sedula
Ahos_0926 Acidianus hospitalis
Saci_1211 Sulfolobus acidocaldarius
ST0830 Sulfolobus tokodaii
PTO0289 Picrophilus torridus
Smar_0546 Staphylothermus marinus
Shell_0249 Staphylothermus hellenicus
Pyrfu_0933 Pyrolobus fumarii
0.4

Fig. 1. Comparative and phylogenetic analysis of the *arn* gene cluster and archaeal vWA proteins.
A. Schematic overview of the *arn* gene cluster in *S. acidocaldarius*. Genes are indicated by arrows and the encoded protein architectures are depicted on top. The FHA domain-containing protein ArnA also incorporates an N-terminal zinc-finger domain.
B. The *arn* gene cluster is conserved across a range of archaeal species and invariably comprises an FHA domain-containing gene and a vWA domain-containing gene in an operon structure, which is flanked upstream by a second copy of a gene encoding a vWA domain-containing protein in the *Sulfolobales*. In some species, the gene cluster additionally comprises a gene encoding a serine/threonine protein phosphatase.
C. Phylogenetic tree indicating that the distribution of the vWA domain proteins is best explained by an ancient gene duplication event at the base of the *Sulfolobales* (depicted with a filled square), followed by lineage-specific gene loss and/or horizontal gene transfer events in the branches leading towards *Metallosphaera* and the euryarchaeon *Picrophilus* (green font). Support values (based on 100 bootstrap replicates) are indicated for each branch, and the tree was rooted with vWA orthologues from the *Desulfurococcales* (blue font).

(Fig. 1B). The presence of related modules in more distant archaeal species suggests that FHA and vWA proteins represent ancient regulatory networks that operate in conjunction with protein phosphatases and protein kinases.

Phosphorylation of ArnA and ArnB

Both genes of the *arn* cluster of *S. acidocaldarius* and the upstream located vWA-encoding gene (*vWA2*, *arnA* and *arnB*) were successfully overexpressed in *Escherichia coli* and the proteins were purified (Fig. S1). The genomic organization to adjacent protein kinases and phosphatases in some species (Fig. 1B) suggested an involvement of these proteins in protein phosphorylation processes. Furthermore, FHA domain-containing proteins were shown to be phosphorylated by ePKs *in vitro* in *M. tuberculosis* and *S. tokodaii* (Grundner *et al.*, 2005; Wang *et al.*, 2010). Therefore *in vitro* phosphorylation studies were performed using [γ-^{32}P]-ATP (Figs 2 and 3). Two kinases of *S. acidocaldarius* (Saci1193 and Saci1694) were tested on autophosphorylation and phosphorylation of ArnA, ArnB and vWA2 since both kinases showed co-occurrence with ArnA in the STRING database (http://string-db.org/). Both kinases showed autophosphorylation activity, which is a common feature of ePKs (Fig. 2A and B, top). This autophosphorylation could be abolished in ATP

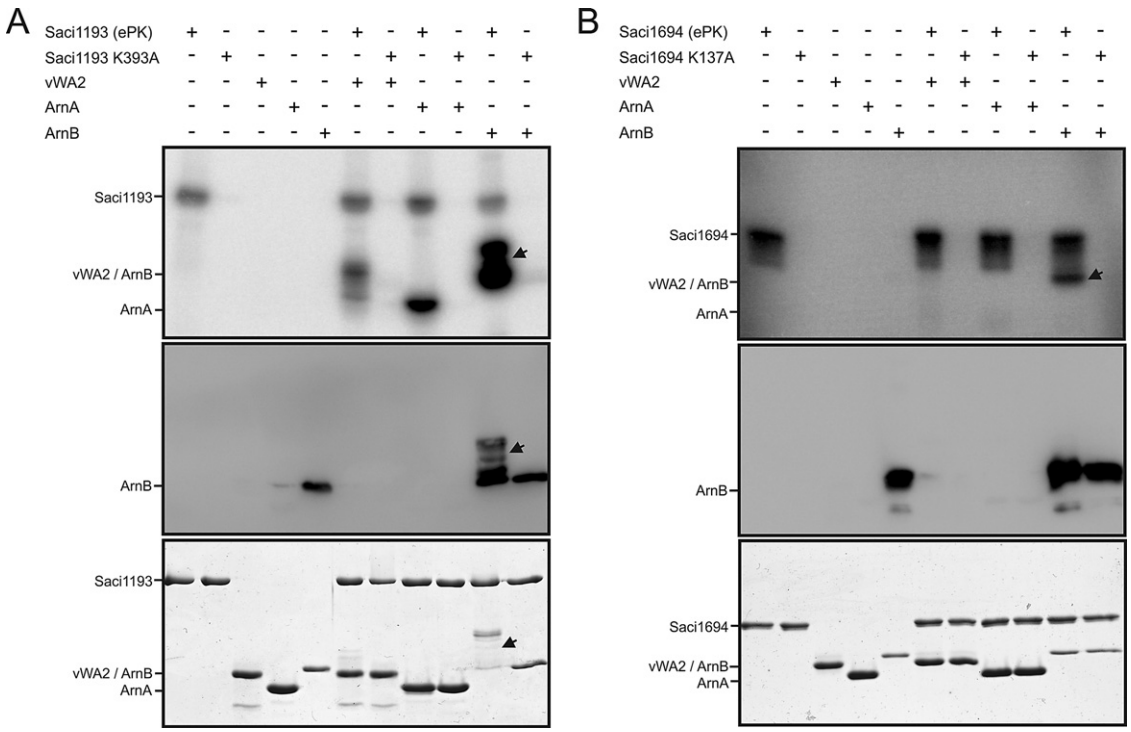

Fig. 2. *In vitro* phosphorylation of ArnA, ArnB and vWA2 by the kinases Saci1193 and Saci1694. Proteins were incubated at 55°C for 30 min with [γ-^{32}P]-ATP. The reaction was stopped with 5× protein loading dye.
A. The ePK Saci1193 phosphorylated all three proteins (ArnA, ArnB and vWA2) *in vitro* (top). To show the upshift (arrow) of ArnB upon phosphorylation more clearly, immunoblotting was performed with specific α-ArnB antibodies (middle). This upshift is also visible on SDS-PAGE (bottom).
B. The ePK Saci1694 specifically phosphorylates ArnB (arrow). To confirm that the phosphorylation is on the height of ArnB and not an effect of the autophosphorylation smear of Saci1694, immunoblotting was performed with specific α-ArnB antibodies (middle) after running SDS-PAGE (bottom).

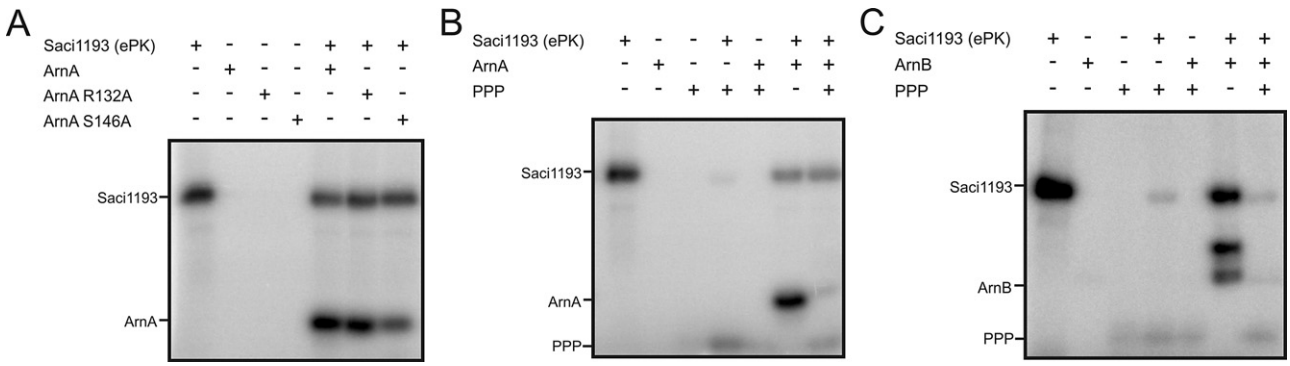

Fig. 3. *In vitro* phosphorylation of ArnA mutants by the kinase Saci1193 and dephosphorylation of ArnA and ArnB with the Ser/Thr phosphatase PPP. Proteins were incubated at 55°C for 30 min with [γ-^{32}P]-ATP. The reaction was stopped with 5× protein loading dye.
A. Different mutants of ArnA, responsible for phosphopeptide interaction of the FHA domain (R132A and S146A), were tested for their phosphorylation behaviour.
B. ArnA could be dephosphorylated by addition of the Ser/Thr phosphatase PPP and incubation for another 10 min.
C. Also ArnB showed a reduced phosphorylation signal upon addition of the Ser/Thr phosphatase PPP.

binding-deficient mutants in which the conserved lysine residue in subdomain II was mutated to an alanine (Fig. 2A and B, top). Furthermore, the experiments revealed phosphorylation of all three proteins encoded in the *arn* cluster by the ePK Saci1193, although ArnB clearly showed the strongest phosphorylation signal (Fig. 2A, top). Upon phosphorylation ArnB running behaviour changes on SDS-PAGE which was clarified with immunoblotting using specific α-ArnB antibodies (Fig. 2A, middle). The second tested ePK, Saci1694, specifically phosphorylated ArnB (Fig. 2B, top). Two mutants of ArnA (R132A and S146A) were also investigated for phosphorylation. These residues are highly conserved among the FHA domains and are involved in phosphopeptide binding (Fig. S2). Both mutants could still be phosphorylated, albeit the $ArnA_{S146A}$ showed a reduced phosphorylation signal (Fig. 3A). Moreover, phosphorylated ArnA and ArnB could be dephosphorylated by the *S. acidocaldarius* Ser/Thr phosphatase PPP (Fig. 3B and C).

Interaction of ArnA and ArnB

arnA and *arnB* are genomically located in a cluster and are both constitutively expressed in the exponential growth phase as well as in the stationary phase (data not shown). Since FHA domain-containing proteins as well as vWA-containing proteins are well known to be involved in protein–protein interactions, the question arose if both proteins interact *in vivo*. Therefore, homologously expressed Strep/His-tagged ArnA and ArnB were purified by Ni-affinity chromatography. In the elution fraction of the purified $ArnA^{Strep/His}$, native ArnB was co-purified as confirmed by Western blot analysis (Fig. 4A) and mass spectrometry. In turn, when $ArnB^{Strep/His}$ was purified, native ArnA was co-eluted (Fig. 4A). This result demonstrates an *in vivo* interaction between the FHA domain-containing protein ArnA and the vWA domain-containing protein ArnB in *S. acidocaldarius*. Interestingly, in the elution fraction no vWA2 protein was detected by mass spectrometry, which confirms specificity of the binding between ArnA and ArnB. Heterologous coexpression on a dual expression vector system (with ArnA Strep-tagged and ArnB His-tagged) in *E. coli* supports the previous result: a strong interaction between $ArnA^{Strep}$ and $ArnB^{His}$ (Fig. 4B).

ArnA and ArnB repress archaellum gene expression

To analyse the *in vivo* function of ArnA and ArnB, in-frame deletion mutants of *vWA2*, *arnA* and *arnB* were constructed in *S. acidocaldarius* MW001 using a single-cross-over pop in/pop out mechanism based on uracil auxotrophy. All deletion mutants were identified by PCR in comparison with the MW001 background strain and confirmed by sequencing (Fig. 5A). All three deletion mutants showed no defect in growth compared with the background strain MW001 (Fig. 5B). It was recently suggested that the *S. tokodaii* ArnA binds in its unphosphorylated state to the *flaX* promoter of the archaellar gene cluster (Duan and He, 2011), indicating a regulatory role in archaellum assembly (Fig. 6A). In *S. acidocaldarius* it was shown that tryptone starvation induced expression of the archaellum and therefore of the structural subunit FlaB as well as of the archaellar component FlaX (Lassak *et al.*, 2012). To test a regulatory role of ArnA and ArnB in archaellum expression, MW001, the Δ*vWA2,* Δ*arnA* and Δ*arnB* deletion strains were subjected to tryptone starvation and the levels of FlaB and FlaX were detected by Western blot analysis. While the expression levels of both FlaB and FlaX, were the same in the wild type as in the Δ*vWA2* deletion strain, their accumulation was significantly higher induced in Δ*arnA* and Δ*arnB* deletion strains (Fig. 6B). The double-deletion strain Δ*arnA*Δ*arnB* showed

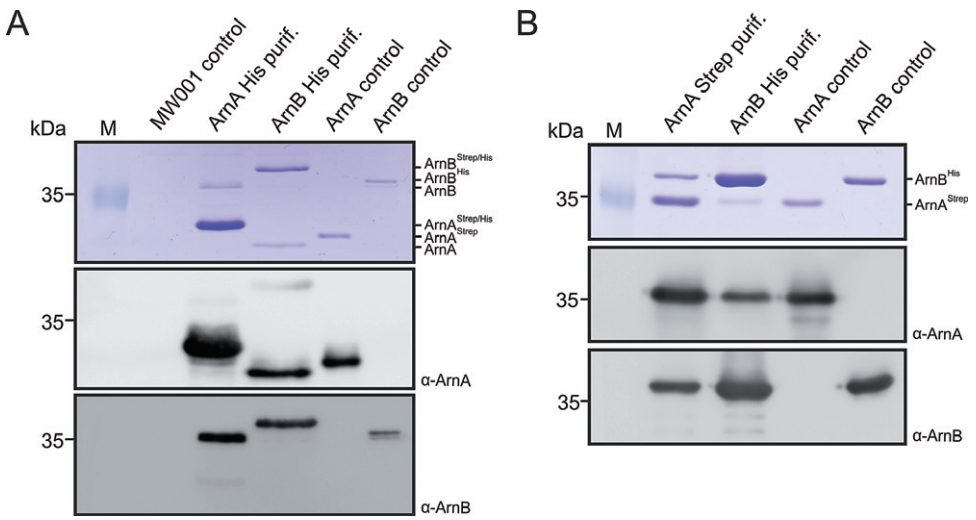

Fig. 4. *In vivo* interaction of ArnA and ArnB.
A. Coomassie-stained SDS-PAGE of the co-purification of ArnA and ArnB homologously expressed in *S. acidocaldarius*. Either ArnA or ArnB was expressed with a Strep/His tag and purified with Ni-affinity chromatography. The different running patterns of the proteins result from the different tags in comparison with the un-tagged native versions. In the elution fractions ArnA and ArnB were identified by specific antibodies using immunoblotting. The control proteins ArnA^{Strep} Strep-tag and ArnB^{His} were expressed in *E. coli*.
B. Coomassie-stained SDS-PAGE of the co-purification of ArnA^{Strep} and ArnB^{His} from heterologous coexpression in *E. coli* by using either a Strep-Tactin column or a Ni-NTA column. In these fractions ArnA and ArnB were identified by specific antibodies using immunoblotting.
M, marker.

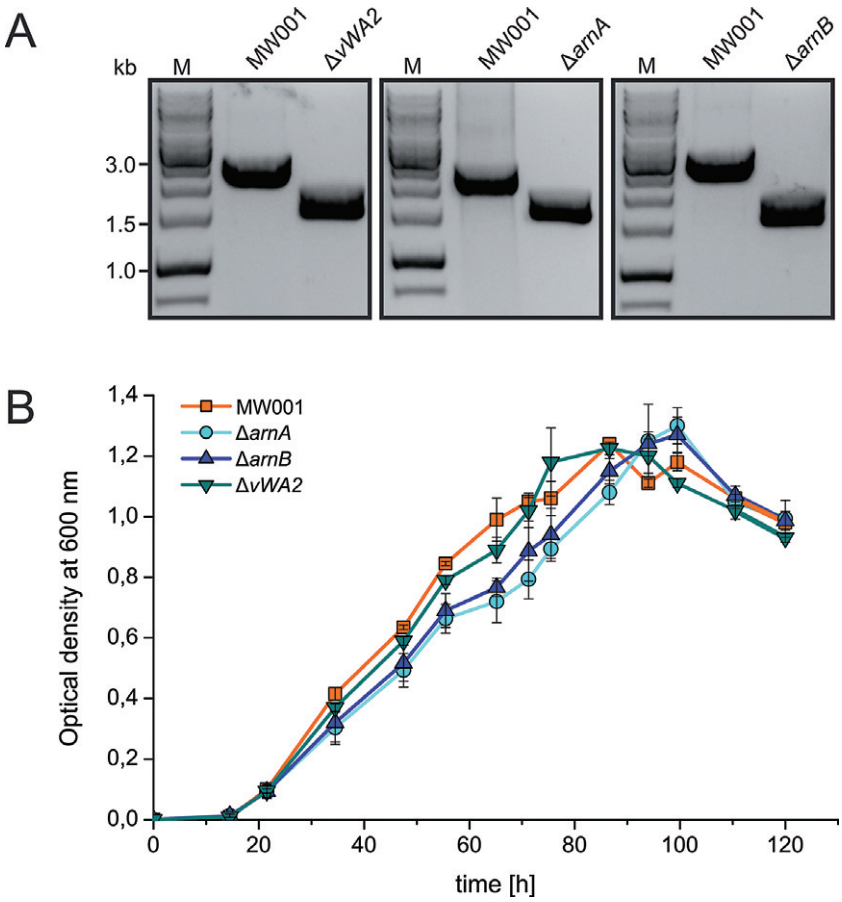

Fig. 5. Confirmation of *vWA2*, *arnA* and *arnB* deletion mutants and determination of growth.
A. Based on a single-cross-over event, deletion mutants of all three genes were constructed in the uracil auxotrophic background strain MW001. The PCR products of the mutants run faster than the wild-type products on agarose gel. M, marker.
B. Growth curve of Δ*vWA2*, Δ*arnA* and Δ*arnB* in comparison with the wt strain MW001. Cells were grown on Brock medium supplemented with 0.1% NZ-amine, 0.2% sucrose and 10 μg ml^{-1} uracil at 76°C. The growth of all strains is comparable.

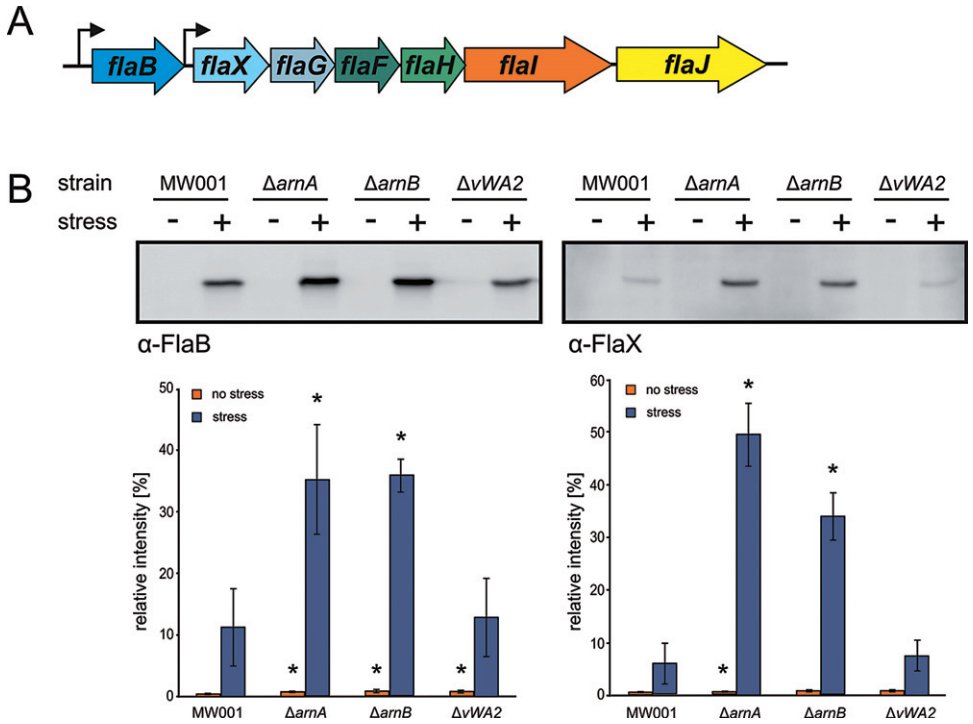

Fig. 6. Expression levels of FlaB and FlaX in MW001, Δ*arnA*, Δ*arnB* and Δ*vWA2*.
A. The archaellum is encoded in an operon consisting of seven genes and two indicated promoter regions in *S. acidocaldarius*.
B. During tryptone-limiting growth conditions archaella expression can be specifically induced. FlaB and FlaX expression levels were detected by immunoblotting with specific antibodies before and after induction via tryptone starvation (top). Four independent stress experiments of the immunoblots were quantified using ImageJ (bottom). The statistical significance in comparison with the wild-type strain MW001 is indicated with a star (*$P < 0.05$).

the same phenotype as the single-deletion mutants (data not shown). These results imply that ArnA and ArnB are repressors of archaellum expression.

To verify the regulatory effect of ArnA and ArnB on archaella expression in *S. acidocaldarius* a motility assay was performed on semi-solid gelrite plates containing reduced amounts of the energy-source NZ-amine (0.005%) to induce starvation. Motility of Δ*arnA* and Δ*arnB* was compared with the motility of MW001 and Δ*aapF*. The latter strain lacks the aap pili which are involved in surface attachment and has been demonstrated to be hypermotile due to an overexpression of the archaellum operon (Henche *et al*., 2012; Lassak *et al*., 2012). After 5 days of incubation at 76°C, the Δ*arnA* and Δ*arnB* cells showed a comparable swimming radius like Δ*aapF*, whereas Δ*vWA2* and MW001 showed almost no motility after this incubation time (Fig. 7A). As described for the Western blot analysis, also in the motility plate assay the double-deletion strain Δ*arnA*Δ*arnB* showed the same phenotype as the single-deletion mutants (Fig. 7A). This hypermotile phenotype could be trans-complemented using a plasmid with the *arnAarnB* operon including the own promoter and terminator regions (Fig. S3).

To further analyse the effect of the *arnA* deletion on motility in *S. acidocaldarius*, the swimming velocity of Δ*arnA* was determined and compared with the wild-type strain MW001 and the hypermotile strain Δ*aapF* (Lassak *et al*., 2012) by thermomicroscopy. Upon tryptone starvation single *S. acidocaldarius* cells were tracked from the recorded movies via ImageJ to determine their swimming velocity. In comparison with the velocity of 30 μm s^{-1} from MW001 and of 48 μm s^{-1} for the hypermotile strain Δ*aapF*, Δ*arnA* swims with an intermediate velocity of 35 μm s^{-1} (Fig. S4). Furthermore, not only the velocity, but also the number of swimming cells under inducing conditions was higher than in the wild type, with about 9% and 31% of swimming cells in MW001 and Δ*arnA* respectively.

Electron microscopy was used to further investigate the influence of ArnA on the production of surface structures in *S. acidocaldarius*. Consistent with the previous data, Δ*arnA* expressed a high level of archaella in tryptone starvation conditions (Fig. 7B). The Δ*arnB* strain did not show this hyperarchaellation effect, but about six times more cells were archaellated. When using an optimized maltose inducible expression system for S. *acidocaldarius* (Berkner *et al*., 2007), overproduction of ArnA resulted in hyper-piliation during normal growth conditions while

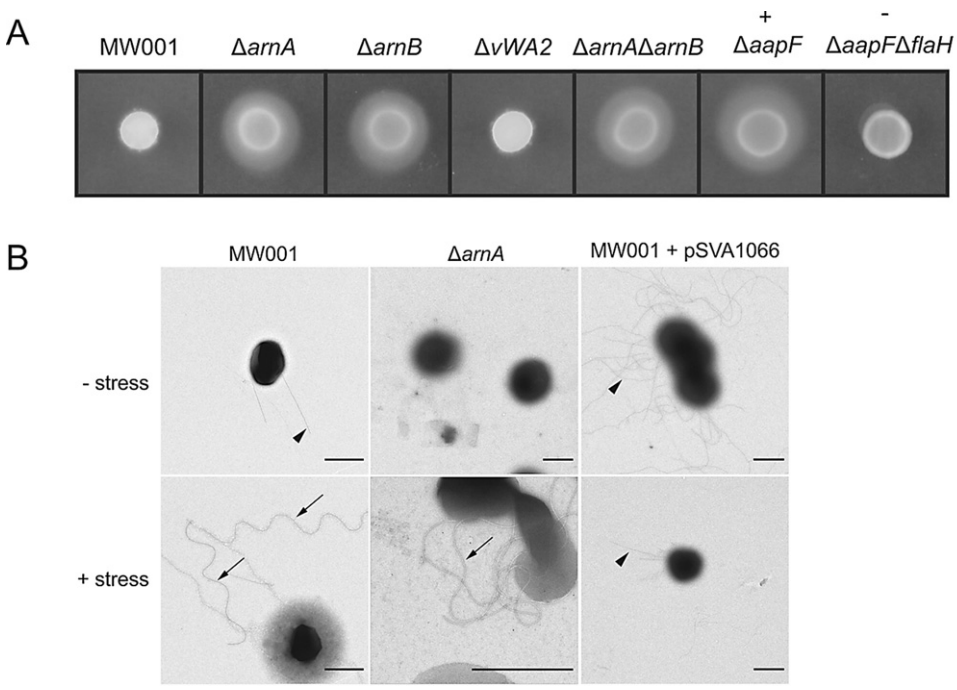

Fig. 7. Motility assay with *S. acidocaldarius* MW001, Δ*arnA,* Δ*arnB,* Δ*vWA2* and the positive (Δ*aapF*) and negative (Δ*flaH*Δ*aapF*) control and electron microscopy.
A. Growing cultures of OD_{600} ~ 1 were spotted on semi-solid gelrite plates with only 0.005% of NZ-amine and were incubated for 5 days at 76°C.
B. Electron micrographs of MW001, Δ*arnA* and MW001 + pSVA1066 (overexpression plasmid for ArnA) during normal growth (– stress) and tryptone starvation (+ stress). Indication of archaella (arrows) and pili (arrowheads). Negative staining with uranyl acetate. Bars: 1 μm.

hardly any archaella were expressed in nutrient-limited conditions (Fig. 7B).

Archaella promoter activity assay

To determine the influence of the *arn* cluster on the archaella promoters p*flaB* and p*flaX*, pSVA1600 and pSVA1601, were transformed into MW001, Δ*arnA,* Δ*arnB* and ΔvWA2 respectively. In pSVA1600 and pSVA1601, the maltose promoter of the reporter gene construct pCMal-LacS was replaced by p*flaB* or p*flaX* (Berkner *et al.*, 2010). The promoter activities driven by *flaB* and *flaX* promoter regions in the different deletion strains were then tested determining LacS activity as described before under optimal and tryptone starved growth conditions (Lassak *et al.*, 2012). In comparison with the wild type the *flaB* promoter was significantly upregulated in Δ*arnA* and Δ*arnB* (Fig. 8A), whereas the *flaX* promoter was more pronounced upregulated in Δ*arnA* under non-inducing and inducing conditions (Fig. 8B). In contrast to the previous

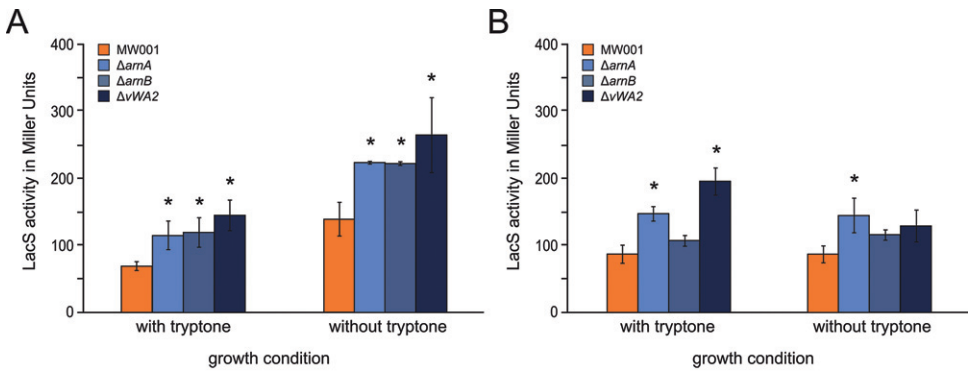

Fig. 8. Promoter activity assay for both *fla* promoters. Reporter gene constructs with *flaB* (A) or *flaX* (B) promoter upstream of *lacS* were transformed into MW001, Δ*arnA,* Δ*arnB*, Δ*vWA2* and Δ*ppp.* The LacS activity was measured based on ONPG conversion and is described as Miller Units. The statistical significance in comparison with the wild-type strain MW001 is indicated with a star (*$P < 0.05$).

results also in Δ*vWA2* both promoters showed an upregulation in both conditions. In total, the influence of the gene deletion was not as high as expected, which leads to the speculation that regulation of the archaellum by ArnA and ArnB is not necessarily based on transcriptional regulation, but could also be based on protein–protein interaction. This observation is also supported by the fact that quantitative RT-PCR did not show higher *flaB* and *flaX* transcript levels in Δ*arnA* in comparison with MW001 under induced conditions (data not shown).

Discussion

Motility is a vital function for most single cellular organisms. In the crenarchaeon *S. acidocaldarius* motility is based on the archaellum (Jarrell and Albers, 2012), which is functionally analogous to the bacterial flagellum and structurally related to type IV pili of Gram-negative bacteria. The crenarchaeal archaellum is encoded in a genomic cluster comprising seven genes, which were shown to be controlled by two promoters in *S. acidocaldarius*, one upstream of the archaellin-encoding gene *flaB* and one upstream of the second gene *flaX* (Lassak *et al*., 2012). In the exponential growth phase archaella gene expression can be specifically induced upon tryptone starvation conditions (Lassak *et al*., 2012). This study provides first insights into the protein modules that underlie the regulation of archaella expression in *S. acidocaldarius*.

Interestingly, among the *Sulfolobales* the *arn* gene cluster genes encoding the FHA protein ArnA and the vWA protein ArnB always localize in each others direct vicinity. The presence of the *arn* gene cluster in *Picrophilus* is best explained by inferring a horizontal gene transfer event from a member of the *Sulfolobales*. Based on the results presented in the current study, it is unlikely that the *arn* genes are involved in cell division related activities, as has been proposed by Makarova *et al*. (2010). Since the *P. torridus* genome lacks archaellum-encoding genes, we suggest that the *arn* genes are part of an alternative regulatory network in this organism.

The conserved clustering of the phosphatase-encoding gene within the *arn* genes in *Sulfolobus solfataricus* and the protein kinase gene in the *Desulfurococcales* suggest a possible involvement of phosphorylation events in modulating the function of ArnA and ArnB. *In vitro* studies revealed phosphorylation of ArnA and ArnB by the ePK Saci1193 and specific phosphorylation of ArnB by the ePK Saci1694. Since FHA domains are well-studied phosphopeptide binding modules, one can speculate if phosphorylation of ArnB is needed for interaction of ArnA with ArnB. However, co-purification revealed a strong interaction of ArnA and ArnB not only in the homologous, but also in the heterologous expression system. Therefore either ArnB can be phosphorylated in *E. coli* or ArnB does not necessarily need to be phosphorylated to interact with ArnA, which will be subject to future studies. ArnA was phosphorylated *in vitro* by the ePK Saci1193. Mutation of the conserved serine, which is involved in phosphopeptide binding in FHA domains, to alanine at position 146 in ArnA led to reduced phosphorylation levels. This suggests that more than one phosphorylation site is present on ArnA, since phosphorylation was not completely abolished. Unfortunately, we were so far unable to determine the phosphorylation sites on ArnA and ArnB by mass spectrometry. For *M. tuberculosis* the FHA protein Rv0020c could not be phosphorylated *in vitro* if the conserved Arg residue, responsible for phosphopeptide binding in the FHA domain, was mutated to an alanine (Grundner *et al*., 2005). In contrast, the R132A mutation in the *S. acidocaldarius* ArnA was still phosphorylated, in line with the results for *S. tokodaii* (Wang *et al*., 2010). This suggests that in the *Sulfolobales* FHA protein phosphorylation is not dependent on phosphopeptide interaction. Since vWA2 was not co-purified with ArnA the phosphorylation pattern of ArnB could lead to specificity in interaction of ArnA and ArnB.

For the first time a negative regulatory effect of ArnA and ArnB on archaella expression was shown *in vivo*. Deletion mutants of *arnA* and *arnB* revealed higher expression levels of FlaB and FlaX, hypermotility on plate, evoked by hyperarchaellation. Since the double-deletion mutant Δ*arnA*Δ*arnB* did not show any additional phenotype than compared with the single mutants, ArnA and ArnB seem to regulate archaella expression at the same hierarchical level, which is in line with the observation that they do interact strongly. Interestingly, the vWA2 protein, which most likely emerged from a gene duplication event of *arnB*, showed no phenotype related to archaella expression in motility assays and protein level analysis, although both *flaB* and *flaX* promoter activities were induced in the Δ*vWA2* deletion strain. Promoter activity assays of *flaB* and *flaX* showed significant but only slightly increased levels of LacS activity in Δ*arnA* and Δ*arnB*. However, the effect is not as high as expected compared with the other *in vivo* assays. For the *S. tokodaii* FHA protein *in vitro* binding to the *flaX* promoter suggested a direct regulation of the archaellum on transcriptional level (Duan and He, 2011). Since the promoter activities were not as high as expected from the *in vivo* results in *S. acidocaldarius*, this might indicate that ArnA and ArnB do not regulate archaella expression on transcriptional level, but possibly on the protein–protein interaction level. The zinc finger domain in ArnA belongs to the RanBP type. Zinc finger domains of this type play a role in RanGDP binding. Therefore, ArnA might be also involved in regulatory processes based on protein interaction in the cell.

ArnA and ArnB could be dephosphorylated *in vitro* by the Ser/Thr phosphatase PPP. Loss of dephosphorylation of ArnA/ArnB could for example lead to a 'constitutive on'

state of archaella expression. However, the loss of repression is only found under nutrient-limiting conditions implicating that another factor is needed that positively induces expression of the archaella operon under starvation conditions. Very recently such a factor was identified in *Sulfolobales* genomes (K. Lassak and S.-V. Albers, unpublished) demonstrating that *S. acidocaldarius* employs a sophisticated regulatory network to regulate and adapt archaella expression to subtle changes in the environment. Furthermore, regulation of archaellum expression (for motility) and aap pili expression (for attachment) might be connected, since overexpression of ArnA lead to hyperpiliation. This hypothesis will be addressed in future studies.

In summary, this study gives first insights into the *in vivo* archaella regulatory processes via ArnA and ArnB and confirms the involvement of phosphorylation events in regulation of archaella expression in *S. acidocaldarius.*

Experimental procedures

Strains and growth conditions

The uracil auxotrophic strain *S. acidocaldarius* MW001 (Wagner *et al.*, 2012) and all markerless deletion mutants were grown in Brock's basal medium (Brock *et al.*, 1972) at pH 3–3.5 and 76°C. Additionally, the medium was supplemented with 0.1% (w/v) tryptone or NZ-amine and 0.2% dextrin, sucrose or maltose.

For heterologous expression of the *S. acidocaldarius* genes, *E. coli* BL21 (DE3) RIL and Rosetta™(DE3)pLysS were used. Propagation of plasmids was conducted in *E. coli* DH5α cells.

Expression of recombinant proteins in E. coli

Luria–Bertani medium (1 l) with 0.4% (w/v) glucose, 50 μg ml^{-1} ampicillin and 30 μg ml^{-1} chloramphenicol was inoculated with 1% of an overnight culture. Cells were grown at 37°C until they reached an OD_{600} of 0.5–0.6 and then induced with 0.5 mM IPTG (isopropyl β-D galactopyranoside). Subsequently the cultures were shifted to 16°C overnight to reduce inclusion body formation. The cells were harvested at 9000 *g* (Beckman Coulter Avanti J-26XP, rotor JLA 8.1), resuspended in lysis buffer (for His-tag purification 50 mM Tris pH 8, 150 mM KCl, 10 mM Imidazole; for Strep-tag purification 100 mM Tris pH 8, 150 mM NaCl), frozen in liquid nitrogen and stored at –80°C until further treatment.

Purification of recombinant proteins in E. coli

Frozen cells were thawed on ice and lysed by sonication (40 min, intensity of 60% and interval of 1 min, Bandelin Sonopuls). Cell debris was removed by low spin centrifugation at 4500 *g* (Thermo Schientific Heraeus Multifuge 3SR+). Membranes were separated with ultracentrifugation at 236 000 *g* for 45 min (Beckman Coulter Optima MAX-XP, rotor MLA-55). To remove most *E. coli* proteins, a heat step was conducted with the soluble fraction at 70°C for 10 min, cooled down on ice and subsequently centrifuged at 236 000 *g* for 30 min. The supernatant was used either for His-tag purification or for Strep-tag purification. For additional purity of the proteins gel filtration was performed (ÄKTA-Purifier, GE Healthcare).

Transformation of plasmids into S. acidocaldarius

Preparation of competent cells, methylation of plasmids and transformation was basically performed as described by Wagner *et al.* (2012). Methylated expression plasmids were transformed into MW001, recovered 30 min at 76°C in Brock medium supplemented with 0.1% NZ-amine and 0.2% sucrose, before plating them on gelrite plates supplemented with 0.1% NZ-amine and 0.2% sucrose.

Expression and purification of proteins in S. acidocaldarius

Four hundred millilitres of Brock medium supplemented with 0.1% NZ-amine and 0.4% D-maltose at pH 3–3.5 was inoculated with 5–10 ml of a 2-day-old *S. acidocaldarius* culture MW001 harbouring the respective expression plasmid. After reaching OD_{600} of 0.7–0.8, cells were harvested by centrifugation at 9100 *g* (Beckman Coulter Avanti J-26XP, rotor JLA 10.5) and resuspended in buffer A (50 mM Tris pH 8, 150 mM KCl, 10 mM imidazole and 1 mM PMSF). Cells were disrupted using sonication (20 min, intensity of 60% and interval 1 min, Bandelin Sonopuls) and cell debris was removed by 15 min centrifugation at 4600 r.p.m. Afterwards membranes were separated from cytoplasm using ultracentrifugation at 250 000 *g* for 45 min (Beckman Coulter Optima MAX-XP, rotor TLA-110). The soluble fraction was used for standard His-tag purification with His-Select Nickel Affinity Gel (Sigma). After binding of the tagged proteins, the column was washed once with 10 column volumes (CV) of buffer A, once with one CV of buffer B (buffer A with 20 mM imidazole) and eluted with three times one CV of buffer C (buffer A with 200 mM imidazole).

Construction of in-frame deletion mutants

The PCR product of about 600–800 bp up- and downstream of the gene of interest were fused via overlap PCR and cloned into the gene targeting plasmid pSVA406 (Wagner *et al.*, 2012). The resulting plasmids were methylated and transformed into *S. acidocaldarius* MW001. Deletion mutants were constructed as described in detail by Lassak *et al.* (2012). In short, after transformation cells were grown on selective gelrite plates for the first and the second selection. Afterwards cultures were screened by colony PCR for the correct clones that were confirmed by sequencing.

Functional and phylogenetic analysis of arn *gene clusters and proteins*

Protein domain analysis was performed using the PFAM database (Punta *et al.*, 2011). The phylogenetic tree of vWA

domain-containing proteins was constructed by multiple sequence alignment of archaeal vWA protein orthologues using MAFFT (v6.84b) (Katoh *et al*., 2005) followed by phylogenetic inference using RAxML (Stamatakis *et al*., 2005) and the LG model of protein evolution (Le *et al*., 2008).

Immunoblotting analysis after nutrient-limited growth conditions

For Western blot analysis of FlaB and FlaX expression cells were tryptone starved. To that end, liquid cultures of *S. acidocaldarius* were grown in Brock medium supplemented with 0.1% tryptone and 0.2% sucrose till an OD_{600} of 0.4–0.6. The cells were centrifuged at 2000 *g* and resuspended in fresh Brock medium without nitrogen and carbon source (stress culture) and with 0.1% tryptone and 0.2% sucrose (control culture). After 5 h of incubation at 76°C, the stressed cells were harvested to equal amounts of cells referring to the OD_{600}. Samples were separated on reducing SDS-PAGE and blotted on a PVDF membrane. The membrane was incubated with a 1:1000 dilution of polyclonal rabbit antibodies against FlaB and FlaX (Eurogentec). After incubation with the alkaline phosphatase coupled goat anti-rabbit secondary antibodies (Sigma), the chemiluminescence of the Western blot was detected with CDP-Star (Roche). Four independent experiments were performed and the relative signal intensity determined using ImageJ (http://rsb.info.nih.gov/ij/docs/menus/analyze.html#gels). The statistical significance of each strain compared with the wild-type MW001 was calculated with Origin 6.1 using independent *t*-test ($P < 0.05$).

Protein interaction study

In the heterologous expression system [*E. coli* BL21(DE3) RIL] pSVA2216 was used for coexpression of His-tagged *arnA* in MCSI and Strep-tagged *arnB* in MCSII of the dual expression vector pETDuet-1 (Novagen). $ArnA^{Strep/His}$ and $ArnB^{Strep/His}$ were expressed homologously in *S. acidocaldarius* MW001 as described above using plasmids pSVA2221 and pSVA2222. Protein purification was conducted as mentioned above with His-Select Nickel Affinity Gel (Sigma). As controls heterologously in *E. coli* expressed $ArnA^{Strep}$ and $ArnB^{His}$ were used. The elution fractions and the control proteins were separated by SDS-PAGE and detected on Western blot with specific antibodies raised in rabbit (Agrisera AB, Sweden) against purified ArnA (1:5000 dilution) and ArnB (1:1000 dilution) heterologously expressed in *E. coli*.

In vitro *phosphorylation assay*

Purified proteins (0.5–3 μM) were assayed in reaction buffer (25 mM MES pH 6.5, 150 mM KCl, 1 mM $MnCl_2$) containing 32 nM [γ-^{32}P]-ATP (222 TBq mmol^{-1}, Hartmann Analytics) and 0.8 mM ATP in a total volume of 15 μl. Proteins were incubated for 30 min at 55°C. The reaction was stopped with the addition of 5× SDS loading dye. The samples were separated by SDS-PAGE and exposed to a Storage Phosphor Screen (Molecular Dynamics) overnight. Images were scanned with Storm 840 scanner.

Motility assay on semi-solid gelrite plates

Strains were grown till OD_{600} of about 0.6–1 and the same amount of cells calculated on OD_{600} were spotted on the semi-solid gelrite plate. The plates containing only 0.15% (w/v) of gelrite were prepared as described before (Lassak *et al*., 2012), supplemented with 0.005% (w/v) tryptone or NZ-amine, 0.2% (w/v) dextrin or sucrose and 10 μg ml^{-1} Uracil in case of the deletion mutants. The plates were incubated for 5 days at 76°C in a metal box (Koerdt *et al*., 2010) with water at the bottom to avoid drying of the plates.

Transmission electron microscopy (TEM)

The same material and the same treatment of cells were used as described in Lassak *et al*. (2012). In short, cells were chemically fixed with 2.5% glutaraldehyde and applied to glow-discharged Carbon-coated 200-mesh copper grids (Plano, Germany). After washing twice with double-distilled water, negative staining with 2% uranyl acetate was conducted for 20 s. Grids were analysed on a JEOL 2100 TEM (JEOL, Tokyo, Japan), equipped with a LaB_6 cathode and a fast-scan 2k × 2k camera F214 (TVIPS, Germany) and operated at 80 kV. The surface appendages were measured in diameter to assign them as pili or archaella.

Thermomicroscopy

For comparison of the swimming velocities of the wild-type strain *S. acidocaldarius* MW001 to the deletion mutant Δ*arnA* the latter was treated and analysed as described by Lassak *et al*. (2012). About 300 cells of each strain were counted to compare the number of swimming cells.

Promoter activity assay

Promoter activity assays for *flaB* and f*laX* promoters were performed basically as described in Lassak *et al*. (2012). Translational promoter fusions were cloned into pCMalLacS (Berkner *et al*., 2010) to exchange the maltose promoter. These plasmids (pSVA1600 and pSVA1601) in addition to the promoterless control plasmid (pSVA1614) were transformed into MW001, Δ*vWA2,* Δ*arnA* and Δ*arnB.* The colour reaction of cleaved o-nitrophenyl-β-D-galactopyranosid (ONPG) by LacS was detected at 410 nm and Miller units were calculated from the assay triplicates. The statistical significance of each strain compared with the wild-type MW001 was calculated with Origin 6.1 using independent *t*-test ($P < 0.05$).

Strains and plasmids

Strain and plasmid lists are shown in *Supporting information* (Tables S1 and S2).

Acknowledgements

We thank Reinhard Wirth (University of Regensburg, Germany) for access to the thermomicroscope. J.R. was

supported by the BMBF project 'SulfoSYS' (0315004C), S.-V.A. by intramural funds of the Max Planck Society and N.Y. by the Chinese Scholar Council. K.L. received funding from the International Max Planck Research School for Environmental, Cellular and Molecular Microbiology.

References

Alatyrev, A.G., Pyatibratov, M.G., Kawarabayasi, Y., Tsujimura, M., Galeva, A.V., and Fedorov, O.V. (2010) Identification of the new protein participating in the archaea motility regulation. *Biochem Mosc Suppl Ser A Membr Cell Biol* **4:** 104–114.

Berkner, S., Grogan, D., Albers, S.-V., and Lipps, G. (2007) Small multicopy, non-integrative shuttle vectors based on the plasmid pRN1 for *Sulfolobus acidocaldarius* and *Sulfolobus solfataricus*, model organisms of the (cren-) archaea. *Nucleic Acids Res* **35:** e88.

Berkner, S., Wlodkowski, A., Albers, S.-V.V., and Lipps, G. (2010) Inducible and constitutive promoters for genetic systems in *Sulfolobus acidocaldarius*. *Extremophiles* **14:** 249–259.

Brock, T.D., Brock, K.M., Belly, R.T., and Weiss, R.L. (1972) *Sulfolobus*: a new genus of sulfur-oxidizing bacteria living at low pH and high temperature. *Arch Mikrobiol* **84:** 54–68.

Colombatti, A., Bonaldo, P., and Doliana, R. (1993) Type A modules: interacting domains found in several non-fibrillar collagens and in other extracellular matrix proteins. *Matrix* **13:** 297–306.

Duan, X., and He, Z.G. (2011) Characterization of the specific interaction between archaeal FHA domain-containing protein and the promoter of a flagellar-like gene-cluster and its regulation by phosphorylation. *Biochem Biophys Res Commun* **407:** 242–247.

Durocher, D., Taylor, I.A., Sarbassova, D., Haire, L.F., Westcott, S.L., Jackson, S.P., *et al.* (2000) The molecular basis of FHA domain:phosphopeptide binding specificity and implications for phospho-dependent signaling mechanisms. *Mol Cell* **6:** 1169–1182.

Dyer, C.M., Vartanian, A.S., Zhou, H., and Dahlquist, F.W. (2009) A molecular mechanism of bacterial flagellar motor switching. *J Mol Biol* **388:** 71–84.

Grundner, C., Gay, L.M., and Alber, T. (2005) *Mycobacterium tuberculosis* serine/threonine kinases PknB, PknD, PknE, and PknF phosphorylate multiple FHA domains. *Protein Sci* **14:** 1918–1921.

Henche, A.-L.L., Koerdt, A., Ghosh, A., and Albers, S.-V.V. (2012) Influence of cell surface structures on crenarchaeal biofilm formation using a thermostable green fluorescent protein. *Environ Microbiol* **14:** 779–793.

Hendrickson, E.L., Liu, Y., Rosas-Sandoval, G., Porat, I., Söll, D., Whitman, W.B., and Leigh, J.A. (2008) Global responses of *Methanococcus maripaludis* to specific nutrient limitations and growth rate. *J Bacteriol* **190:** 2198–2205.

Hofmann, K., and Bucher, P. (1995) The FHA domain: a putative nuclear signalling domain found in protein kinases and transcription factors. *Trends Biochem Sci* **20:** 347–349.

Jarrell, K.F., and Albers, S.-V. (2012) The archaellum: an old motility structure with a new name. *Trends Microbiol* **20:** 307–312.

Katoh, K., Kuma, K., Toh, H., and Miyata, T. (2005) MAFFT version 5: improvement in accuracy of multiple sequence alignment. *Nucleic Acids Res* **33:** 511–518.

Koerdt, A., Gödeke, J., Berger, J., Thormann, K.M., Albers, S.-V.V., and Godeke, J. (2010) Crenarchaeal biofilm formation under extreme conditions. *PLoS ONE* **5:** e14104.

Lassak, K., Neiner, T., Ghosh, A., Klingl, A., Wirth, R., and Albers, S.V. (2012) Molecular analysis of the crenarchaeal flagellum. *Mol Microbiol* **83:** 110–124.

Le, S.Q., Lartillot, N., and Gascuel, O. (2008) Phylogenetic mixture models for proteins. *Philos Trans R Soc Lond B Biol Sci* **363:** 3965–3976.

Makarova, K.S., Yutin, N., Bell, S.D., and Koonin, E.V. (2010) Evolution of diverse cell division and vesicle formation systems in Archaea. *Nat Rev Microbiol* **8:** 731–741.

Mukhopadhyay, B., Johnson, E.F., and Wolfe, R.S. (2000) A novel pH2 control on the expression of flagella in the hyperthermophilic strictly hydrogenotrophic methanarchaeaon *Methanococcus jannaschii*. *Proc Natl Acad Sci USA* **97:** 11522–11527.

Pennell, S., Westcott, S., Ortiz-Lombardia, M., Patel, D., Li, J., Nott, T.J., *et al.* (2010) Structural and functional analysis of phosphothreonine-dependent FHA domain interactions. *Structure* **18:** 1587–1595.

Pohlschroder, M., Ghosh, A., Tripepi, M., and Albers, S.-V. (2011) Archaeal type IV pilus-like structures – evolutionarily conserved prokaryotic surface organelles. *Curr Opin Microbiol* **14:** 357–363.

Punta, M., Coggill, P.C., Eberhardt, R.Y., Mistry, J., Tate, J., Boursnell, C., *et al.* (2011) The Pfam protein families database. *Nucleic Acids Res* **40:** 290–301.

Rudolph, J., and Oesterhelt, D. (1996) Deletion analysis of the *che* operon in the archaeon *Halobacterium salinarium*. *J Mol Biol* **258:** 548–554.

Rudolph, J., Tolliday, N., Schmitt, C., Schuster, S.C., and Oesterhelt, D. (1995) Phosphorylation in halobacterial signal transduction. *Eur Mol Biol Organ J* **14:** 4249–4257.

Sadler, J.E., Shelton-Inloes, B.B., Sorace, J.M., Harlan, J.M., Titani, K., and Davie, E.W. (1985) Cloning and characterization of two cDNAs coding for human von Willebrand factor. *Proc Natl Acad Sci USA* **82:** 6394–6398.

Schlesner, M., Miller, A., Streif, S., Staudinger, W.F., Müller, J., Scheffer, B., *et al.* (2009) Identification of Archaea-specific chemotaxis proteins which interact with the flagellar apparatus. *BMC Microbiol* **9:** 56.

Stamatakis, A., Ludwig, T., and Meier, H. (2005) RAxML-III: a fast program for maximum likelihood-based inference of large phylogenetic trees. *Bioinformatics* **21:** 456–463.

Tuckwell, D. (1999) Evolution of von Willebrand factor A (VWA) domains. *Biochem Soc Trans* **27:** 835–840.

Wagner, M., Van Wolferen, M., Wagner, A., Lassak, K., Meyer, B.H., Reimann, J., and Albers, S.-V. (2012) Versatile genetic tool box for the crenarchaeote *Sulfolobus acidocaldarius*. *Front Microbiol* **3:** 214.

Wang, B., Yang, S.F., Zhang, L., and He, Z.G. (2010) Archaeal eukaryote-like serine/threonine protein kinase

interacts with and phosphorylates a forkhead-associated-domain-containing protein. *J Bacteriol* **192:** 1956–1964.
Welch, M., Oosawa, K., Aizawa, S., and Eisenbach, M. (1993) Phosphorylation-dependent binding of a signal molecule to the flagellar switch of bacteria. *Proc Natl Acad Sci USA* **90:** 8787–8791.
Whittaker, C.A., and Hynes, R.O. (2002) Distribution and evolution of von Willebrand/integrin A domains: widely dispersed domains with roles in cell adhesion and elsewhere. *Mol Biol Cell* **13:** 3369–3387.

Supporting information

Additional supporting information may be found in the online version of this article.

Please note: Wiley-Blackwell are not responsible for the content or functionality of any supporting materials supplied by the authors. Any queries (other than missing material) should be directed to the corresponding author for the article.

Supplementary material of

"Regulation of Archaella Expression by the FHA and von Willebrand Domain-Containing Proteins ArnA and ArnB in *Sulfolobus acidocaldarius*"

Julia Reimann, Kerstin Lassak, Sunia Khadouma, Thijs J. G. Ettema, Nuan Yang, Arnold J. M. Driessen, Andreas Klingl and Sonja-Verena Albers

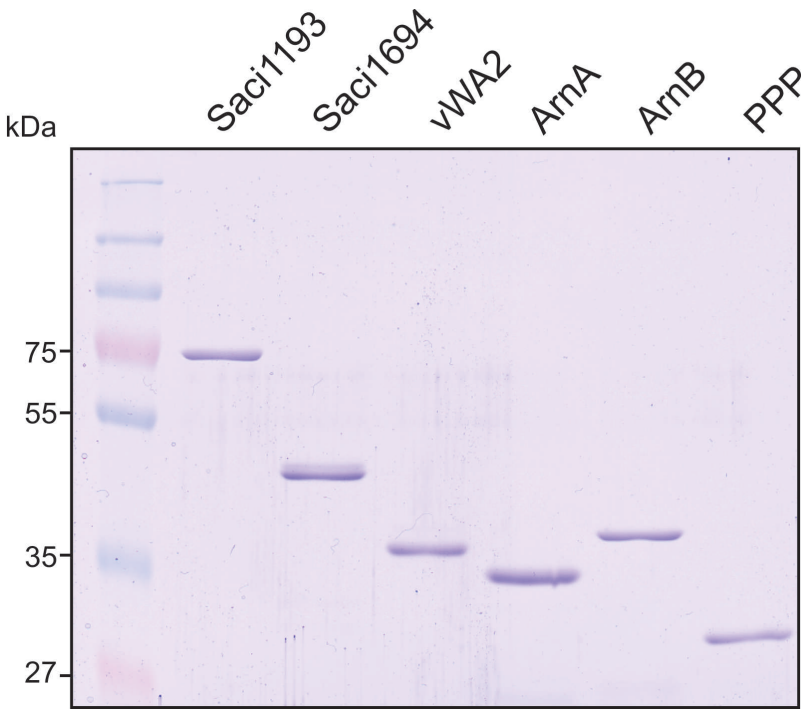

Figure S1

Figure S1. Expression and purification of the kinases Saci1193 and Saci1694, ArnA, ArnB vWA2, and the phosphatase PPP. All proteins were expressed in *E. coli* BL21 (DE3) RIL or Rosetta (DE3) pLysS with an IPTG inducible T7 promoter. The proteins were purified either via Ni-NTA column or via Strep-Avidin column depending on the tag. Increased purity was obtained with gel filtration.

Figure S2

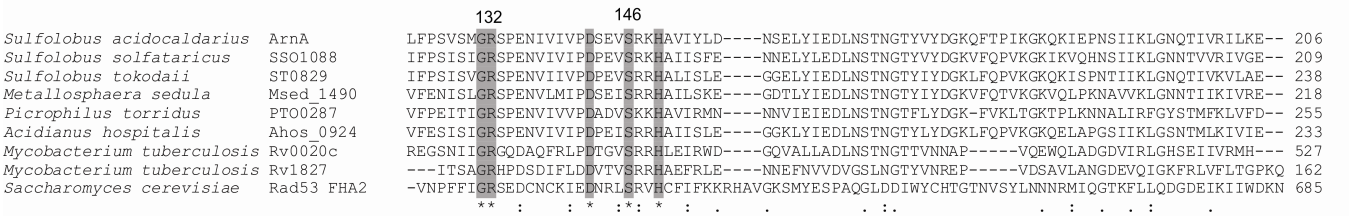

Figure S2. Alignment of FHA-domains from different organisms. The most conserved amino acid residues of the FHA domains are colored in gray. The numbers above indicate the amino acid position in ArnA that were mutated to an alanine residue.

Figure S3

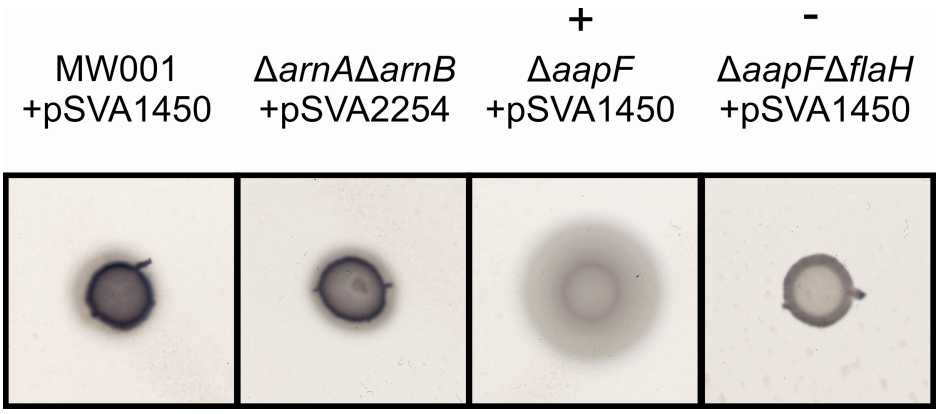

Figure S3. Motility assay of the trans-complemented hypermotile strain Δ*arnA*Δ*arnB*. Strains were grown for five days on semi-solid gelrite plates with 0.005 % NZ-Amine and 0.2% D-maltose, but without Uracil. Δ*arnA*Δ*arnB* was transformed with pSVA2254 containing the *arnAarnB*-operon with its own promoter and terminator region. The control strains (Δ*aapF* and Δ*aapF*Δ*flaH*) and the background strain MW001 were transformed with the expression vector pSVA1450 to be able to grow without uracil. The hypermotile phenotype of Δ*arnA*Δ*arnB* was complemented and showed motility comparable to MW001.

Figure S4

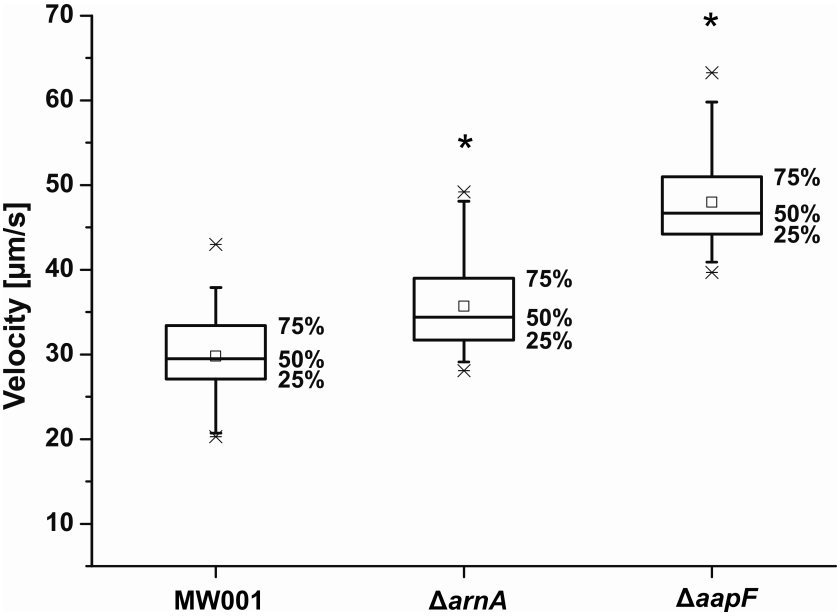

Figure S4. Swimming velocities of MW001, Δ*arnA* and Δ*aapF*. Swimming velocities were determined by tracking and evaluating single cell movement from thermomicroscopy movies via ImageJ. The diagram shows a box plot, in which the middle 50 % of the values are depicted in the box. The line shows the median and the square indicates the mean value, while the star (*) shows the significance in comparison to the wild type strain. The *arnA* deletion strain has an intermediate velocity (35 µm s^{-1}) compared to the background strain MW001 and the hypermotile strain Δ*aapF.*

Table S1. Primers used in this study.

primer	sequence (5´ - 3´)	purpose
	primers for pSVA1031	
1575	GGGCCATGGCTCTCCTGGAGGGATATTTC	Δ*saci1210* upstr fw *Nco*I
1576	ATAAACTCACTCCTTCCACGTCATACACGTAATATTCTG	Δ*saci1210* upstr rev ol
1577	ACGTGTATGACGTGGAAGGAGTGAGTTTATGACCATA	Δ*saci1210* downstr fw ol
1578	GGGGGATCCATCTCGCCATACACTCTTAC	Δ*saci1210* downstr rev *BamH*I
1634	TAGCTTACCTCGTTGATCAC	Δ*saci1210* check primer fw
1635	CGCTTTACATCATTTGCTCTTG	Δ*saci1210* check primer rev
	primers for pSVA1062	
1579	GGGCCATGGGCTTACCCTAACTATCAAAC	Δ*saci1211* upstr fw *Nco*I
1580	CCTTGTTTAAGACCTTATGGTCATAAACTCACTCCTT	Δ*saci1211* upstr rev ol
1581	GAGTTTATGACCATAAGGTCTTAAACAAGGACTAAATTTATC	Δ*saci1211* downstr fw ol
1582	GGGGATCCGTAGACATTGAAGAAGGTAAAG	Δ*saci1211* downstr rev *Bam*HI
1636	ATCTACTTGCTGAAGACAATG	Δ*saci1211* check primer fw
1637	GAACAGGGAGAGGACTTC	Δ*saci1211* check primer rev
	primers for pSVA1069	
3118	GGACCATGGCCTGAGGGTGAATCTGGCAAAC	Δ*saci1209* upstr fw *Nco*I
1645	GTTACCATAATACCTGAGTCAGTCTATCATAACAACGTAATG	Δ*saci1209* upstr rev ol
1646	TACGTTGTTATGATAGACTGACTCAGGTATTATGGTAACCTTATATC	Δ*saci1209* downstr fw ol
1647	GGTGGATCCAGCCACTCGTCATTAATTAG	Δ*saci1209* downstr rev *Bam*HI
1669	ACAGACCCTACACCCTTCTC	Δ*saci1209* check primer fw
1670	GGTATCCTGCTCAATAGTTC	Δ*saci1209* check primer rev
	primers for pSVA2217	
1575	GGGCCATGGCTCTCCTGGAGGGATATTTC	Δ*saci1210* upstr fw *Nco*I
3178	TCCTTGTTTAAGACCTCCACGTCATACACGTAATATTCTG	Δ*saci1210* Δ*saci1211* upstr rev ol
3179	ACGTGTATGACGTGGAGGTCTTAAACAAGGACTAAATTTATC	Δ*saci1210* Δ*saci1211* downstr fw ol
1582	GGGGATCCGTAGACATTGAAGAAGGTAAAG	Δ*saci1211* downstr rev *Bam*HI
1634	TAGCTTACCTCGTTGATCAC	Δ*saci1210* check primer fw

1637	GAACAGGGAGAGGACTTC	Δ*saci1211* check primer rev
	primers for pSVA1009	
1507	GGGGTGATCAGGATTTAGCATTCGTTAAG	Saci1193 expr. fw *Bcl*I
1508	GGGCTGCAGTTAGATCTCTGAGTAGTTAA	Saci1193 expr. rev *Pst*I
	primers for pSVA1076	
1648	GGGCCATGGAAAGTAGTAGTGTATC	Saci1694 expr. fw *Nco*I
1649	GGGCTGCAGTTAGTGGTGATGATGGTGATGTTTCTTCTCTGCTCTTTGTAATAAGTC	Saci1694 expr. rev *Pst*I with His-tag
	primers for pSVA1034	
1614	GGGAGGGCATATGACGTGGAAATGTAATTTATGC	Saci1210 expr. fw *Nde*I
1594	GGGCCTAGGTTACTTCTCAAATTGTGGATGACTCCACTCCTTTAATATTCGTACTATTGTCTGATTACC	Saci1210 expr. rev *Avr*II with Strep-tag
	primers for pSVA1036	
1597	GGGCCATGGCTACCATATCAGTTAAAGCCGAATTAAG	Saci1211 expr. fw *Nco*I
1598	GGGGGATCCTTAGTGGTGATGATGGTGATGAGACCTCAACTTCTTAGTAACTTCACTAG	Saci1211 expr. rev *Bam*HI with His-tag
	primers for pSVA1068	
1642	GGACCATGGCCACAGTTAGCGTTTCTTTAAAATC	Saci1209 expr. fw *Nco*I
1643	GGCGGATCCTGTCCTCATTGTTTTTGTAACTTC	Saci1209 expr. rev *Bam*HI
	primers for pSVA2216	
	Same as pSVA1034 and pSVA1036 in one plasmid	
	primers for pSVA1037	
1599	GGGCCATGGCTAACATTGAAGAAACGTATGAG	Saci0884 expr. fw *Nco*I
1600	GGGGGATCCTTAGTGGTGATGATGGTGATGTACTATCTCTTCTATTAGTTGATCGTTCAC	Saci0884 expr. rev *Bam*HI with His-tag
	primers for pSVA2234	
3133	GTTTGCCATGGCGATAGTGAAGAAAGAG	Saci1193 K_{393}A fw ol
3134	CTTCACTATCGCCATGGCAAACTTTCTCATG	Saci1193 K_{393}A rev ol
	primers for pSVA2238	
3141	GTTAGCAGTAGCGATCTACAGGCTCGAG	Saci1694 K_{137}A fw ol
3142	CCTGTAGATCGCTACTGCTAACTTATTAGC	Saci1193 K_{137}A rev ol
	primers for pSVA2246	
3149	ATCAATGGGTGCGAGTCCTGAAAAC	Saci1210 R_{132}A fw ol
3150	TTCAGGACTCGCACCCATTGATACAC	Saci1210 R_{132}A rev ol
	primers for pSVA2247	
3151	TTCAGAAGTAGCTAGAAAACACGCAG	Saci1210 S_{146}A fw ol

3152	GTGTTTTCTAGCTACTTCTGAATCAGG	Saci1210 S_{146}A rev ol
	primers for pSVA1035	
1595	GGGCCATGGCTACGTGGAAATGTAATTTATGC	Saci1210 hom. expr. fw *Nco*I
1596	GGGGGATCCCTCCTTTAATATTCGTACTATTG	Saci1210 hom. expr. rev *Bam*HI
	primers for pSVA2220	
1597	GGGCCATGGCTACCATATCAGTTAAAGCCGAATTAAG	Saci1211 hom. expr. fw *Nco*I
3187	GGGGGATCCAGACCTCAACTTCTTAGTAACTTC	Saci1211 hom. expr. rev *Bam*HI
	primers for pSVA2254	
3236	AGGCCGCGGATCTACTTGCTGAAGACAATG	Δ*saci1210_1211* complement. fw *Sac*II
3237	AGGCGGCCGTACGACGAGAAGGATAATACAG	Δ*saci1210_1211* complement. rev *Eag*I

Table S2. Strains and plasmids used in this study.

Strains	Genotype	Source/ Reference
Strains		
DH5α	*Escherichia coli* K-12 cloning strain l2 f80d/*lacZ*D*M15* D(*lacZYA-argF*)*U169 recA1 endA1 hsdR17* (rK2 mK1) *supE44 thi-1 gyrA relA1*	Gibco
BL21 (DE3)	*Escherichia coli* expression strain	Stratagene
RIL	B F- *ompT* hsdS(rB- mB-) *dcm+* Tetr *E. coli* gal λ (DE3) *endA* Hte [*argU ileY leuW* Camr]	
Rosetta (DE3)	*Escherichia coli* expression strain	Merck
pLysS	F^- *ompT* $hsdS_B(r_{B^-}\ m_{B^-})$ *gal dcm* (DE3) pLysSRARE (Cam^R)	
ER1821	*Escherichia coli* propagation strain F^- *glnV44 e14*$^-$*(McrA*$^-$*) rfbD1? relA1? endA1 spoT1? thi-1* Δ*(mcrC-mrr)114::IS10*	New England Biolabs
MW001	*Sulfolobus acidocaldarius* DSM639 Δ*pyrE*	(Wagner et al., 2012)
MW351	MW001 Δ*saci1210* (Δ*arnA*)	This work
MW353	MW001 Δsaci*1211* (Δ*arnB*)	This work
MW356	MW001 Δ*saci1209* (Δ*vWA2*)	This work
MW376	MW001 Δ*saci1210*Δ*saci1211* (Δ*arnA*Δ*arnB*)	This work
MW156	MW001 Δ*saci2318* (Δ*aapF*)	(Henche, Koerdt, Ghosh, & Albers, 2012)
MW455	MW001 Δ*saci2318*Δ*saci1174* (Δ*aapF*Δ*flaH*)	(Lassak et al., 2012)
Plasmids		
pSVA406	Gene targeting plasmid, pGEM-T Easy backbone, $pyrEF_{SSO}$ cassette; single crossover method	(Wagner et al., 2012)
pSVA407	Gene targeting plasmid, pGEM-T Easy backbone, $pyrEF_{SSO}$ and $lacS_{SSO}$ cassette; single crossover method	(Wagner et al., 2012)
pΔ2*pyrEF*	Gene targeting plasmid, pBluescript backbone, $pyrEF_{SSO}$; single crossover method	(Wagner et al., 2009)
pSVA1031	In-frame deletion of *saci1210* (*arnA*) cloned into pSVA406 with *Nco*I, *Bam*HI	This work
pSVA1062	In-frame deletion of *saci1211* (*arnB*) cloned into pSVA407 with *Nco*I, *Bam*HI	This work
pSVA1069	In-frame deletion of *saci1209* (*vWA2*) cloned into pSVA406 with *Nco*I, *Bam*HI	This work
pSVA2217	In-frame deletion of *saci1210* (*arnA*) and *saci1211* (*arnB*) cloned into pSVA406 with *Nco*I, *Bam*HI	This work
pETDuet-1	Amp^r, Car^r, expression plasmid containing replicon ColE1 (pBR322) and two MCS (MCS1 and MCS2)	Novagen
pSA4	Derivative of pET15b containing the multiple cloning site and C-terminal hexa-His tag of pSA5	(Albers, Szabó, & Driessen, 2003)
pSVA1009	*saci1193* with N-terminal His-tag cloned into pETDuet-1 with *Bcl*I/*Bam*HI, *Pst*I into MCSI	This work
pSVA1076	*saci1694* with C-termial His-tag cloned into pETDuet-1 with *Nco*I, *Pst*I in MCSI	This work
pSVA1034	*saci1210* with C-terminal Strep-tag cloned into pETDuet-1 with *Nde*I, *Avr*II in MCSII	This work
pSVA1036	*saci1211* with C-termial His-tag cloned into pETDuet-1 with *Nco*I, *Bam*HI in MCSI	This work
pSVA1068	*saci1209* with C-termial His-tag cloned into pSA4 with *Nco*I, *Bam*HI	This work
pSVA2216	*saci1211* with C-termial His-tag cloned into pETDuet-1 with *Nco*I, *Bam*HI in MCSI and *saci1210* with C-terminal Strep-tag cloned into pETDuet-1 with *Nde*I, *Avr*II in MCSII	This work
pSVA1037	*Saci0884* with C-termial His-tag cloned into pETDuet-1 with	This work

	*Nco*I, BamHI in MCSI	
pSVA2234	*saci1193* K393A with N-terminal His-tag in pETDuet-1 mutated from pSVA1009	This work
pSVA2238	*saci1694* K137A with C-termial His-tag in pETDuet-1 mutated from pSVA1076	This work
pSVA2246	*saci1210* R132A with C-terminal Strep-tag in pETDuet-1 mutated from pSVA1034	This work
pSVA2247	*saci1210* S146A with C-terminal Strep-tag in pETDuet-1 mutated from pSVA1034	This work
pSVA2254	*saci1210_1211* with own promoter and stop region for complementation of Δ*saci1210*Δ*1211* (MW376)	This work
pMZ1	*E. coli* entry vector with *ara*-promoter and C-terminal Strep- and His-tag	(Zolghadr, Weber, Szabo, Driessen, & Albers, 2007)
pCMalLacS	pRN-1 based shuttle vector with $lacS_{sso}$ reporter gene	(Berkner, Wlodkowski, Albers, & Lipps, 2010)
pSVA1481	*E. coli* entry vector with *ara*-promoter and C-terminal Strep- and His-tag based on pGEM-T Easy backbone and pMZ1 cassette	Wagner & Albers, unpublished
pSVA1450	Plasmid for expression in *S. acidocaldarius* based on pCMalLacS with *mal* promoter	Wagner & Albers, unpublished
pSVA1035	*saci1210* cloned into pMZ1 with *Nco*I, *Bam*HI	This work
pSVA2220	*saci1211* cloned into pSVA1481 with *Nco*I, *Bam*HI	This work
pSVA1066	*saci1210* cloned from pSVA1035 into pCMalLacS with *Nco*I, *Eag*I	This work
pSVA2222	*saci1210* cloned from pSVA1035 into pSVA1450 with *Nco*I, *Eag*I	This work
pSVA2221	*saci1211* cloned from pSVA2220 into pSVA1450 with *Nco*I, *Eag*I	This work
pSVA1600	*flaB* promoter replacing *mal* promoter, cloned into pCMalLacS with *Sac*II, *Nco*I	(Lassak et al., 2012)
pSVA1601	*flaX* promoter replacing *mal* promoter, cloned into pCMalLacS with *Sac*II, *Nco*I	(Lassak et al., 2012)
pSVA1614	pClacS, promoterless vector for negative control in promoter activity assay	(Lassak et al., 2012)

References

Albers, S.-V., Szabó, Z., & Driessen, A. J. M. (2003). Archaeal homolog of bacterial type IV prepilin signal peptidases with broad substrate specificity. *Journal Of Bacteriology*, *185*(13), 3918-3925.

Berkner, S., Wlodkowski, A., Albers, S.-V. V., & Lipps, G. (2010). Inducible and constitutive promoters for genetic systems in *Sulfolobus acidocaldarius*. *Extremophiles*, *14*(3), 249-259.

Henche, A.-L. L., Koerdt, A., Ghosh, A., & Albers, S.-V. V. (2012). Influence of cell surface structures on crenarchaeal biofilm formation using a thermostable green fluorescent protein. *Environ Microbiol*, *14*(3), 779-793.

Lassak, K., Neiner, T., Ghosh, A., Klingl, A., Wirth, R., & Albers, S. V. (2012). Molecular analysis of the crenarchaeal flagellum. *Mol Microbiol*, *83*(1), 110-124.

Wagner, M., Berkner, S., Ajon, M., Driessen, A. J. M., Lipps, G., & Albers, S.-V. (2009). Expanding and understanding the genetic toolbox of the hyperthermophilic genus *Sulfolobus*. *Biochemical Society Transactions*, *37*(Pt 1), 97-101.

Wagner, M., van Wolferen, M., Wagner, A., Lassak, K., Meyer, B. H., Reimann, J., & Albers, S.-V. (2012). Versatile genetic tool box for the crenarchaeote *Sulfolobus acidocaldarius. Frontiers in Microbiology*, *3, 214.*

Zolghadr, B., Weber, S., Szabo, Z., Driessen, A. J., & Albers, S. V. (2007). Identification of a system required for the functional surface localization of sugar binding proteins with class III signal peptides in *Sulfolobus solfataricus*. *Mol Microbiol*, *64*(3), 795-806.